Kinetic and X-Ray Structural Studies of a Mutant *Escherichia coli* Alkaline Phosphatase (His-412 → Gln) at One of the Zinc Binding Sites[†,‡]

Lan Ma and Evan R. Kantrowitz*

Department of Chemistry, Merkert Chemistry Center, Boston College, Chestnut Hill, Massachusetts 02167

Received October 2, 1995; Revised Manuscript Received December 7, 1995[⊗]

ABSTRACT: Site-specific mutagenesis has been used to replace His-412 with glutamine in *Escherichia coli* alkaline phosphatase. In the wild-type enzyme His-412 is a direct ligand to one of the catalytically important zinc atoms (Zn_1) in the active site. The mutant enzyme (H412Q) exhibited about the same k_{cat}, but a 50-fold increase in K_m compared to the corresponding kinetic parameters for the wild-type enzyme. Furthermore, the H412Q enzyme had a lower zinc content than the wild-type enzyme. In contrast to the wild-type enzyme, Tris was less effective in the transferase reaction and dramatically inhibited the hydrolysis reaction of the H412Q enzyme. The addition of zinc to the mutant enzyme increased the k_{cat} value above that of the wild-type enzyme, partially restored the weak substrate and phosphate binding, and also alleviated the inhibition by Tris. The structure of the H412Q enzyme was also determined by X-ray crystallography. The overall structure of the H412Q enzyme was very similar to that of the wild-type enzyme; the only α-carbon displacements over 1 Å were observed near the mutation site. In the H412Q structure no phosphate was bound in the active site of the enzyme; however, two water molecules were observed where phosphate normally binds in the wild-type enzyme. Close examination of the active site of the H412Q structure revealed structural changes in Ser-102 as well as at the mutation site. For example, the carbonyl oxygen of the side chain of Gln-412 rotated away from the position of His-412 in the wild-type structure, although too far away (3.2 Å) to coordinate to Zn_1. Studies on the H412Q enzyme, and a comparison of the H412Q and H412N structures, suggest that the structure and electrostatics of the imidazole ring of histidine are critical for its function as a zinc ligand in alkaline phosphatase.

Alkaline phosphatase (EC 3.1.3.1), a nonspecific phosphomonoesterase, functions through a phosphoseryl intermediate (E−P) (Engström, 1962, Schwartz & Lipmann, 1961) to produce an alcohol (ROH) and inorganic phosphate (P_i) in a hydrolysis reaction or to transfer the phosphate to an acceptor (R′OH) such as ethanolamine or Tris (Dayan & Wilson, 1964; Wilson et al., 1964) in a transferase reaction (Scheme 1). In the enzyme-catalyzed reaction, the rate-limiting step is pH dependent. At acidic pH, the hydrolysis of the covalent enzyme−phosphate complex (E−P) is rate limiting, while at alkaline pH, the dissociation of the noncovalent enzyme−phosphate complex (E·P_i) is rate limiting (Hull et al., 1976).

Alkaline phosphatase is a dimeric metalloenzyme containing one magnesium and two zinc atoms in each active site. The enzyme from *Escherichia coli* has been extensively studied [for a review, see Coleman (1992)] and the X-ray structure has been solved and refined to 2.0 Å resolution (Kim & Wyckoff, 1991; Sowadski et al., 1983, 1985). In the *E. coli* enzyme, the metal binding sites M1 and M2 are usually occupied by zinc and the M3 site by magnesium. The two zinc atoms are directly involved in catalysis, whereas magnesium does not directly participate in the mechanism but is important for the structure of the active site (Anderson et al., 1975, 1976; Janeway et al., 1993, Plocke & Vallee, 1962; Simpson & Vallee, 1968). Zn_1[1] is absolutely required for catalysis and plays an important role in binding both the substrate and phosphate. A metal-assisted double in-line displacement mechanism has been proposed for *E. coli* alkaline phosphatase with the direct involvement of Zn_1 (Kim & Wyckoff, 1991). The X-ray structure of the *E. coli* enzyme shows that the phosphate or the phosphate portion of substrate is held by Zn_1 as well as Zn_2 and Arg-166 (Figure 1) (Kim & Wyckoff, 1991). In the structure of the wild-type enzyme, Zn_1 is in close proximity to the other

Scheme 1

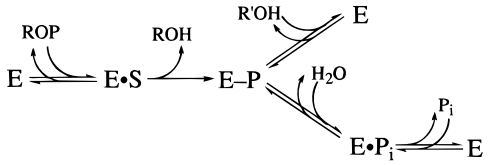

† Supported by Grant GM42833 from the National Institute of General Medical Sciences and by Pittsburgh Supercomputing Center Grant 1 P41 RR06009 from the NIH National Center for Research Resources.

‡ The coordinates for the H412Q alkaline phosphatase have been deposited in the Protein Data Bank (1HQA).

* To whom correspondence should be addressed.

⊗ Abstract published in *Advance ACS Abstracts,* February 1, 1996.

[1] Abbreviations: TMZP buffer, 0.01 M Tris, 0.001 M $MgCl_2$, 10^{-5} M $ZnSO_4$, 10^{-4} M NaH_2PO_4, 0.31 × 10^{-2} M NaN_3, pH 7.4 (Bloch & Beckar, 1978); TMP buffer, TMZP buffer without $ZnSO_4$; H412Q, the mutant alkaline phosphatase that has His-412 replaced by Gln; P_i, inorganic phosphate; RMSD, root-mean-square deviation; Zn_1, Zn_2, and Mg sites correspond to the M1, M2, and M3 sites as identified in the X-ray structure of the wild-type enzyme (Sowadski et al., 1983); Zn_1, Zn^{2+} bound in the M1 site of alkaline phosphatase; Zn_2, Zn^{2+} bound in the M2 site of alkaline phosphatase; Mg, Mg^{2+} bound in the M3 site of alkaline phosphatase; H412N(−Zn), the structure of the H412N enzyme determined with crystals that did not have zinc added to the stabilization buffer; H412N(+Zn), the structure of the H412N enzyme determined with crystals soaked in stabilization buffer containing 10 mM zinc chloride.

0006-2960/96/0435-2394$12.00/0

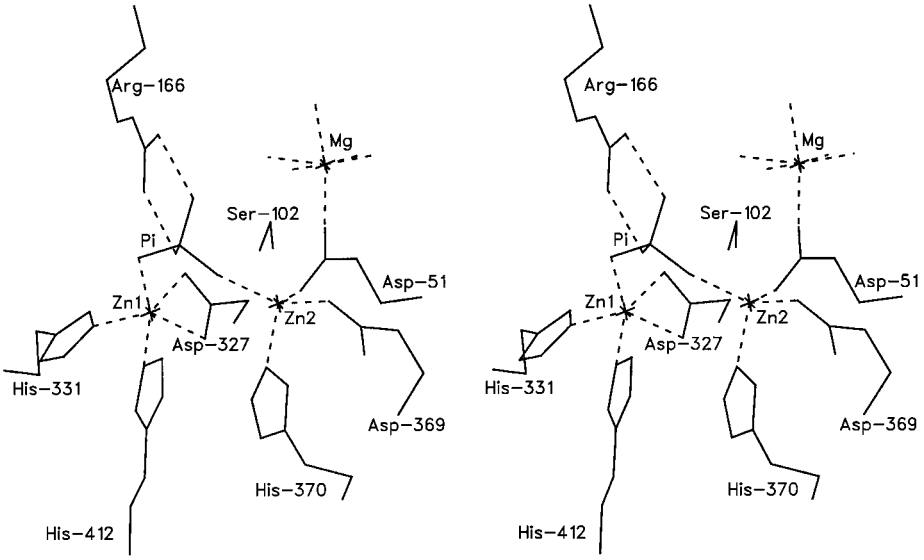

FIGURE 1: Active site of *E. coli* alkaline phosphatase. Shown are Zn_1, Zn_2, phosphate (P_i), and their ligands as well as Mg^{2+}. Zn_1 interacts with imidazole nitrogens of His-412 and His-331, one of the phosphate oxygens, and the carboxylate oxygens of Asp-327. Zn_2 interacts with the imidazole nitrogen of His-370, one of the phosphate oxygens, and the carboxylate oxygens of Asp-51 and Asp-369. For clarity, the ligands to the Mg are not shown. Also shown are Ser-102, which is phosphorylated during the reaction, and Arg-166, which interacts with the phosphate.

two metal sites; therefore, any changes at the Zn_1 site could affect the rest of the active site.

Site-specific mutagenesis has been used as a tool to probe the metal binding sites in *E. coli* alkaline phosphatase. His-412 in the wild-type enzyme interacts directly with Zn_1 through its imidazole nitrogen (Kim & Wyckoff, 1991). To study the specificity of the interaction between His-412 and Zn_1 in alkaline phosphatase as well as the nature of histidine as a metal ligand found in many enzymes, we replaced His-412 by Asn or Ala through site-specific mutagenesis (Ma & Kantrowitz, 1994). These studies indicated that neither Asn or Ala could effectively replace His as a ligand to Zn_1. The substitutions of His by Asn and Ala produced enzymes with low catalytic efficiency, low substrate affinity, reduced zinc affinity, and inhibition rather than activation by Tris. The X-ray structure of the H412N enzyme showed changes at the phosphate and the Zn_1 sites (Ma et al., 1995). The side chain of Asn-412 was observed to be in a position similar to that of the side chain of His-412 in the structure of the wild-type enzyme; however, Asn-412 was not coordinated to Zn_1. Here we report the kinetic characterization and X-ray structural determination of the mutant version of alkaline phosphatase in which His-412 has been replaced by Gln (H412Q). This study will provide further understanding of the role of His-412 in alkaline phosphatase and, in particular, the specificity of the interaction between His-412 and Zn_1.

EXPERIMENTAL PROCEDURES

Materials

Agar, agarose, ampicillin, chloramphenicol, *p*-nitrophenyl phosphate, sodium dihydrogen phosphate, magnesium chloride, and zinc chloride were purchased from Sigma Chemical Co. Tris, ethanolamine, enzyme-grade ammonium sulfate, and sucrose were supplied by ICN Biomedicals. Tryptone and yeast extract were from Difco Laboratories. All the reagents needed for DNA sequencing were obtained from US Biochemicals. Restriction endonucleases, T4 DNA ligase, T4 DNA polymerase I, and T4 polynucleotide kinase were from either US Biochemical or New England Biolabs and used according to the supplier's recommendations. DNA fragments were isolated from agarose gels with the Geneclean II kit from Bio 101 Inc.

Strains. The *E. coli* K12 strain MV1190 [Δ(*lac-proAB*), *supE*, *thi*, Δ(*sri-recA*) 306::Tn10(tet^r)/F′ *traD36*, *proAB*, *lacI*^{q}, *lacZ*ΔM15] and the M13 phage M13K07 were obtained from J. Messing. The Δ*phoA E. coli* K12 strain SM547 [Δ(*phoA-phoC*), *phoR*, tsx::Tn5, Δ*lac*, *galK*, *galU*, *leu*, str^r] was a gift of H. Inouye. The strain CJ236 [*dut-1*, *ung-1*, *thi-1*, *relA-1*/pCJ105(Cm^r)] was a gift of T. Kunkel.

Oligonucleotide Synthesis. The oligonucleotides required for the site-specific mutagenesis and the sequencing primers were synthesized on an Applied Biosystems 381A DNA synthesizer and purified by HPLC employing a DuPont Zorbay Oligo ion-exchange column.

Methods

Construction of the H412Q Alkaline Phosphatase by Site-Specific Mutagenesis. The mutation of His-412 to Gln was introduced by the method of Kunkel (1985, 1987) with modifications (Chaidaroglou et al., 1988; Vieira & Messing, 1987; Xu & Kantrowitz, 1991). Confirmation of the mutation was accomplished by DNA sequence analysis. Once a mutant candidate was identified, a small DNA fragment containing the mutation was cut out and inserted into pEK48 which had the corresponding wild-type fragment removed. The H412Q mutation in the newly constructed plasmid, pEK203, was verified by DNA sequence analysis.

Expression and Purification of the Wild-Type and Mutant Alkaline Phosphatases. Both the wild-type and mutant alkaline phosphatases were expressed in the host strain SM547 transformed with the plasmids pEK48 and pEK203, respectively. Both enzymes were purified using the same procedure as described previously (Chaidaroglou et al., 1988). SDS gel electrophoresis was used to judge the purity of the enzyme (Laemmli, 1970).

Determination of Protein Concentration. The wild-type enzyme concentration was measured by its absorbance at

280 nm with an extinction coefficient of 0.71 cm^2/mg (Plocke & Vallee, 1962). The concentration of the mutant enzyme was determined using the Bio-Rad version of Bradford's dye binding assay (Bradford, 1976) or the Lowry method (Lowry et al., 1951) with the wild-type enzyme as the standard.

Steady-State Kinetics. The velocity of the enzyme-catalyzed reaction was measured spectrophotometrically at 410 nm using *p*-nitrophenyl phosphate as substrate at 25 °C by monitoring the release of *p*-nitrophenolate (Garen & Levinthal, 1960). The extinction coefficient of *p*-nitrophenolate was determined by measuring the absorbance after complete hydrolysis of a known amount of substrate. The sum of hydrolysis and transferase activities was determined using 1.0 M Tris-HCl as the reaction buffer, while the hydrolysis activity alone was determined using 0.01 M Tris-HCl. The ionic strength of these buffers was held constant at 0.5 with NaCl.

^{31}P NMR. Spectra were recorded on a Varian Unity 500 spectrometer at 202.3 MHz with a broad band probe. The reactions were carried out in 1.0 and 0.5 M Tris buffer at pH 8 or 10, with or without added zinc as indicated, at an initial concentration of *p*-nitrophenyl phosphate of 30 mM. Between 0.02 and 0.1 mg of either the wild-type or the H412Q enzyme was added to 1.0 mL of the reaction mixture. The reactions were monitored at 410 nm and stopped by separating enzyme from the substrate by ultrafiltration when about 60% of the substrate had been converted to products.

Zinc Determination. The zinc content of the wild-type and the mutant enzymes was determined with a Perkin Elmer 3100 atomic absorption spectrophotometer using the stabilized temperature platform furnace technique. Before the measurements, the enzymes were extensively dialyzed against TMP buffer.

Crystallization. Crystals were obtained using the hanging vapor diffusion method. Before use, the enzyme, at a concentration of approximately 30 mg/mL, was dialyzed against a buffer composed of 20% saturated $(NH_4)_2SO_4$, 100 mM Tris, 10 mM $MgCl_2$, and 0.01 mM $ZnCl_2$ at pH 9.5. Protein drops of 15 μL were suspended on cover slips and equilibrated with 1 mL of buffer [44% saturating $(NH_4)_2SO_4$, 100 mM Tris, 10 mM $MgCl_2$ at pH 9.5]. The crystals, which grew in 2−3 weeks, were harvested by transferring them to a stabilization solution containing 55% saturated $(NH_4)_2SO_4$, 100 mM Tris, 10 mM $MgCl_2$, 10 mM $ZnCl_2$, and 2 mM NaH_2PO_4 at pH 7.5, and soaked for several days before data collection.

Data Collection and Processing. The diffraction data were collected with an Area Detector Systems MARK III system at the Crystallographic Facility in the Chemistry Department of Boston College. The area detector system was controlled by a Micro VAX3500 computer for data collection using a Rigaku RU-200 rotating-anode X-ray generator operated at 50 kV and 150 mA. The instrumental setup has been reported previously (Tibbitts et al., 1994). The data were collected to 2.25 Å resolution. A total of 170 722 measurements were obtained, of which 58 551 were unique reflections giving an average redundancy of 2.9. The diffraction data were merged and processed by using the software provided by Area Detector Systems (Hamlin et al., 1981).

Structural Refinement. The coordinates of the wild-type *E. coli* alkaline phosphatase (Brookhaven Data Bank file 1ALK) were used as the starting point for structural refinement, with metals, phosphate, and waters removed. In addition, His-412 was replaced by Gln using QUANTA (Molecular Simulations, Inc. Burlington, MA). The structure was refined using X-PLOR (Brünger, 1992, Molecular Simulations, Inc.) running on Silicon Graphics Indigo II workstations at Boston College and on the Cray Y-MP C90 at the Pittsburgh Supercomputer Center. The initial *R* factor was 0.35. Subsequent cycles of positional refinement and temperature factor refinement improved the *R* factor and stereochemistry. At this stage, the metals, their water ligands, and phosphate were built in according to the calculated $(2F_o - F_c)$ and $(F_o - F_c)$ electron density maps using QUANTA. The structures were then further refined by cycles of positional refinement, temperature factor refinement, and simulated annealing using initial temperatures up to 3000 °C. An initial set of solvent water molecules were then added from the D369N structure (Tibbitts et al., 1994, Brookhaven Data Bank file 1ALH). During subsequent refinement the temperature factors of the waters were carefully monitored. Water molecules with temperature factors above 60 Å^2 were deleted, except for the waters in the second coordination shell, for which the temperature factors were kept under 70 Å^2. At several stages, additional solvent water molecules were added based upon difference Fourier maps $(F_o - F_c)$. During refinement noncrystallographic symmetry constraints (Tibbitts et al., 1994) were used. Simulated annealing omit maps (Brünger, 1992) were also used to determine the positions of side chains in the active site region of this structure.

Table 1: Kinetic Parameters of the Wild-Type and H412Q Enzymes[a]

enzyme	k_{cat}[b] (s^{-1})	K_m (μM)	$k_{cat}/K_m \times 10^{-6}$ ($M^{-1}\cdot s^{-1}$)	K_i[c] (μM)
	(A) In the Absence of a Phosphate Acceptor[d]			
wild-type	38 (±1)	4 (±1)	9.5	10 (±2)
H412Q	39 (±2)	200 (±30)	0.195	230 (±40)
	(B) In the Presence of a Phosphate Acceptor[e]			
wild-type	81 (±1)	16 (±1)	5.1	
H412Q	2.8 (±0.2)	$>3 \times 10^4$[f]	$<9.3 \times 10^{-5}$	

[a] Kinetic data were determined at 25 °C with *p*-nitrophenyl phosphate as substrate at pH 8.0. Both the wild-type and the H412Q enzymes were dialyzed versus TMP buffer before use. [b] The k_{cat} values are calculated from the V_{max} by use of a dimer molecular weight of 94 000 (Bradshaw, 1981). The k_{cat} per active site is half of the value indicated. [c] The K_i values were determined by the method of Segel (1975) which takes into account the fact that the product of the reaction is also an inhibitor. The theoretical equation was fit to the data by nonlinear least-squares. [d] 0.01 M Tris was used as reaction buffer adjusted to pH 8.0 with HCl, and the ionic strength to 0.5 with NaCl. [e] 1.0 M Tris was used as reaction buffer; the pH was adjusted to 8.0 with HCl. [f] The value of the K_m for the mutant enzyme is approximate because the very low activity of this enzyme makes K_m determination difficult.

RESULTS

Steady-State Kinetics of the Wild-Type and Mutant Enzymes at pH 8.0 in the Absence and Presence of a Phosphate Acceptor. The kinetic analyses of the wild-type and H412Q enzymes were first performed using 0.01 M Tris, pH 8.0, as the reaction buffer. Under these conditions, only the hydrolysis activity of the enzyme is measured. The mutant enzyme showed the same k_{cat} but a 50-fold increase in K_m compared to the value for the wild-type enzyme (Table 1). The activity was then determined in 1.0 M Tris buffer, pH 8.0. Under these conditions, the rate observed for the wild-

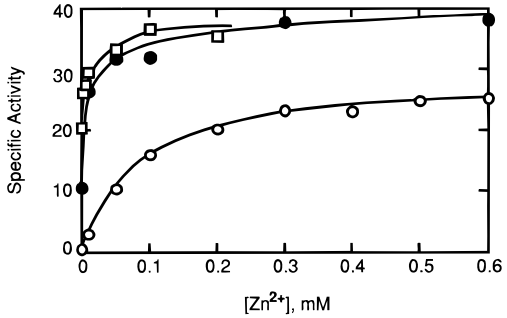

FIGURE 2: Influence of Zn^{2+} on the specific activity of the H412Q enzyme in 1.0 M Tris (○), 1.0 M ethanolamine (●), and 0.01 M Tris (□). Assays were carried out at 25 °C with 0.6 mM *p*-nitrophenyl phosphate as substrate at pH 8.0. Before use the enzyme was dialyzed against TMP buffer.

type enzyme is the sum of the transphosphorylation and hydrolysis reactions since Tris can serve as a phosphoryl group acceptor. Therefore, it was expected that the activity should be the same as or greater than the activity measured in the absence of a phosphate acceptor. However, the mutant enzyme had very low activity in the presence of 1.0 M Tris, in fact 14-fold lower than the value in the absence of a phosphate acceptor (Table 1). The K_m of the H412Q enzyme increased dramatically compared to the value for the wild-type enzyme.

Zinc Content of the Wild-Type and Mutant Enzymes. Since His-412 is a direct ligand to Zn_1, the replacement of His-412 by Gln might be expected to alter the zinc affinity of the mutant enzyme. Therefore, the residual zinc content of the H412Q enzyme was measured and compared to the value for the wild-type enzyme determined under identical conditions. After being dialyzed against buffer without zinc, the zinc contents of the wild-type and H412Q enzymes were determined by atomic absorption spectrophotometry. The wild-type enzyme contained 3.3 ± 0.4 mol of zinc per mol of enzyme dimer, while the H412Q enzyme contained 1.7 ± 0.2 mol of zinc per mol of enzyme dimer.

Effects of Zinc on the Steady-State Kinetics of the Wild-Type and Mutant Enzymes at pH 8.0 in the Absence and Presence of a Phosphate Acceptor. Since the replacement of His-412 by Gln resulted in an enzyme with lower zinc content compared to the wild-type enzyme, the dependence of the activity on zinc concentration was determined in both 0.01 M and 1.0 M Tris buffer, as well as in 1.0 M ethanolamine, another phosphate acceptor. The activity of the H412Q enzyme increased with increasing zinc concentration (Figure 2), while the zinc concentration had almost no effect on the activity of the wild-type enzyme. The optimal concentrations of Zn^{2+} required for activation of the H412Q enzyme were about 0.6 mM Zn^{2+} in 1.0 M Tris, 0.3 mM in 1.0 M ethanolamine, and 0.1 mM in 0.01 M Tris. The k_{cat} and K_m values for the H412Q enzyme with the addition of 0.6 mM Zn^{2+} in 1.0 M Tris were dramatically improved, compared to the corresponding values in the absence of Zn^{2+} (Tables 1 and 2). In 0.01 M Tris, with 0.1 mM Zn^{2+}, the k_{cat} of the H412Q enzyme was slightly higher than the wild-type value while the K_m was 6-fold higher than the wild-type value. Since the enzyme used in these studies was dialyzed before use to remove loosely bound zinc, the zinc activation of the H412Q enzyme most likely reflects the higher zinc occupancy.

Table 2: Kinetic Parameters of the Wild-Type and H412Q Enzymes in the Presence of Zn^{2+} [a]

enzyme	k_{cat}[b] (s^{-1})	K_m (μM)	$k_{cat}/K_m \times 10^{-6}$ ($M^{-1}\cdot s^{-1}$)	K_i[c] (μM)
	(A) In the Absence of a Phosphate Acceptor[d]			
wild-type	41 (±1)	3.3 (±0.4)	12.4	15 (±4)
H412Q	55 (±1)	27 (±3)	2.0	39 (±7)
	(B) In the Presence of a Phosphate Acceptor[e]			
wild-type	81 (±2)	17 (±2)	4.8	
H312Q	47 (±1)	390 (±20)	0.12	

[a] Kinetic data were determined at 25 °C with *p*-nitrophenyl phosphate as substrate at pH 8.0. Both the H412Q and the wild-type enzymes were dialyzed versus TMP buffer before use. [b] The k_{cat} values are calculated from the V_{max} by use of a dimer molecular weight of 94 000. The k_{cat} per active site would be half of the value indicated. [c] The K_i values were determined by the method of Segel (1975), which takes into account the fact that the product of the reaction is also an inhibitor. The theoretical equation was fit to the data by nonlinear least-squares. 0.1 mM Zn^{2+} was added to the reaction mixture. [d] 0.01 M Tris was used as reaction buffer adjusted to pH 8.0 with HCl and the ionic strength to 0.5 with NaCl. 0.1 mM Zn^{2+} was added to the reaction mixture. [e] 1.0 M Tris was used as reaction buffer; the pH was adjusted to 8.0 with HCl. 0.6 mM Zn^{2+} was added to the reaction mixture.

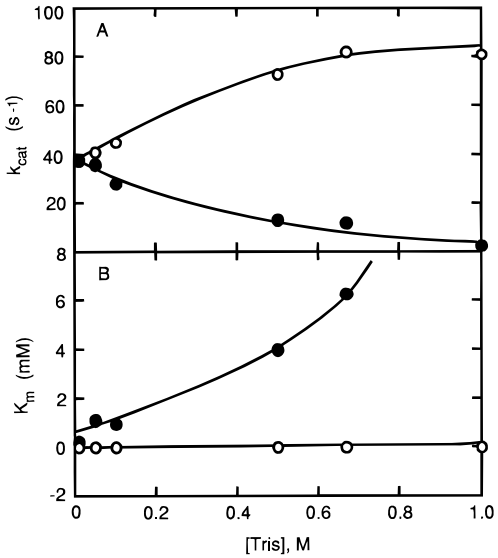

FIGURE 3: Effect of Tris concentration on the k_{cat} (A) and the K_m (B) for the wild-type (○) and the H412Q (●) enzymes. All reactions were carried out at pH 8 and 25 °C. The enzymes were treated as reported in the legend to Figure 2.

Tris Effect on the Steady-State Kinetics of the Wild-Type and Mutant Enzymes at pH 8.0. To investigate further how Tris influenced the activity of the H412Q enzyme, kinetic parameters were measured as a function of Tris concentration. For the wild-type enzyme, the K_m remained constant and the k_{cat} increased with increasing concentrations of Tris. However, Tris inhibited the activity of the H412Q enzyme at all concentrations of Tris employed; furthermore, the inhibition increased as the Tris concentration increased (Figure 3). This inhibition could be partially eliminated by the addition of zinc (Table 2).

^{31}P NMR experiments were carried out with both the wild-type and the H412Q enzymes to investigate the effect of Tris on the hydrolysis and transferase activities. From the NMR spectra of the transferase reaction product, O-Tris phosphate, and the hydrolysis reaction product P_i, the ratio between the transferase and hydrolysis reactions could be determined (Figure 4). For the wild-type enzyme, in 1.0 M

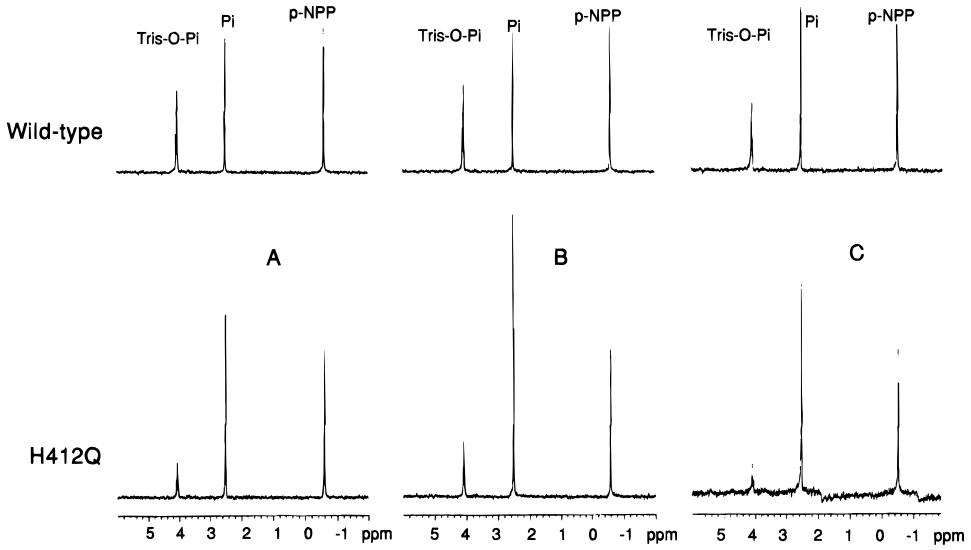

FIGURE 4: ^{31}P NMR spectra of products from reactions catalyzed by the wild-type (upper panel) and the H412Q enzymes (lower panel). The reactions were carried out at pH 8 in (A) 1.0 M Tris without zinc, (B) 1.0 M Tris with 0.6 mM Zn^{2+}, and (C) 0.5 M Tris without zinc.

Table 3: Summary of the Data Collection and Refinement Statistics for the H412Q Alkaline Phosphatase

(A) Data Collection

enzyme form	space group	d_{min} (Å)	reflections (total, unique)	completeness	redundancy	unit cell (Å)	overall R_{merge}[a]
H412Q	I222	2.25	170 722, 58 551	98%	2.9	$a = 194.9$ $b = 167.0$ $c = 76.8$	0.080

(B) Refinement Statistics

					RMS deviations from ideal values		
enzyme form	final R factor	d_{min} (Å)	metals and phosphate present	waters	bond lengths (Å)	bond angles	improper dihedral angles
H412Q	0.16	2.25	Zn_1, Zn_2, Zn_3,[b] P_i	389	0.02	2.0°	1.7°

[a] $R_{merge} = \sum_{hkl}\sum_i|I_{mean} - I_i|/\sum_{hkl}\sum_i I_i$. [b] The third metal site appeared to be occupied by zinc.

Tris buffer, pH 8, with or without 0.6 mM Zn^{2+}, the ratio between the transferase and hydrolysis reactions was about the same at 1.3:1, whereas in 0.5 M Tris buffer, pH 8, without Zn^{2+}, the ratio decreased to about 1:1. For the H412Q enzyme, in 1.0 M Tris buffer, pH 8, without zinc or in the presence of 0.6 mM Zn^{2+}, the ratio between the transferase and the hydrolysis reactions was about 0.5:1. In 0.5 M Tris buffer, pH 8, without zinc, the ratio decreased slightly to approximately 0.44:1.

Phosphate Inhibition. Inorganic phosphate is not only a product of the alkaline phosphatase reaction but also is a competitive inhibitor of the enzyme. To measure the strength of phosphate binding to the wild-type and mutant enzymes, the phosphate inhibition constant K_i was determined at pH 8.0 (Segel, 1975) in 0.01 M Tris in the absence or presence of 0.1 mM $ZnCl_2$ (Tables 1 and 2). In the absence of Zn^{2+}, phosphate bound weakly to the H412Q enzyme as compared to the wild-type enzyme; however, the phosphate affinity increased with the addition of Zn^{2+}. The K_i value decreased 7-fold in the presence of 0.1 mM Zn^{2+} compared to the value in the absence of Zn^{2+}. At this zinc concentration, the K_i of phosphate was within 3-fold of the wild-type value.

Structure of the H412Q Alkaline Phosphatase. The H412Q enzyme crystallized in the same space group and with unit cell dimensions similar to those found in crystals of the wild-type enzyme with one molecule in the asymmetric unit (Table 3). The structure was refined to an R factor of 0.16 at a resolution of 2.25 Å with reasonable stereochemistry. As seen in Figure 5, the overall structure of the H412Q enzyme was very similar to that of the wild-type enzyme (Kim & Wyckoff, 1991), with the only α-carbon displacement over 1 Å observed near the mutation site. The average RMS displacements between the H412Q and wild-type structures were 0.17 Å for the α-carbons and 0.44 Å for the side chain positions. A Luzatti plot of the resolution dependence of the crystallographic R factor (Figure 6) indicated that the uncertainty in the coordinates of this structure was approximately 0.20 Å (Luzatti, 1952). Of a total of 892 residues in the two subunits, 99.7% were within

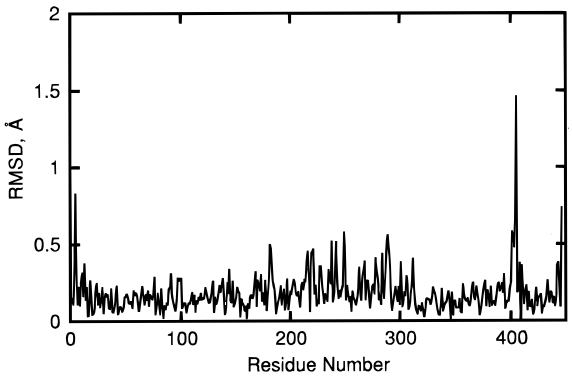

FIGURE 5: Root-mean-square displacements (RMSD) between the positions of α-carbon atoms of the H412Q and the wild-type structures. Data shown here are for the B-chain.

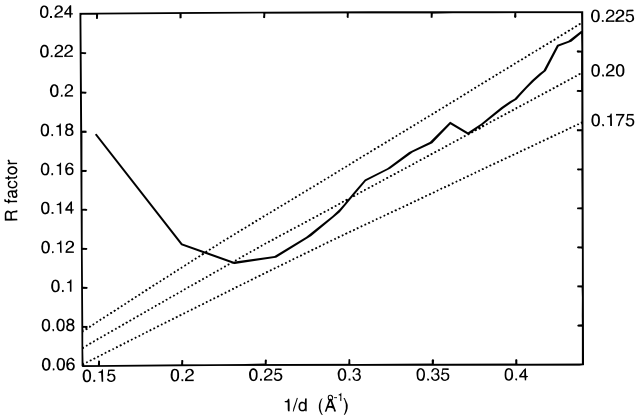

FIGURE 6: Luzatti plot showing the final crystallographic *R* factors, by resolution shell, for the H412Q enzyme. The expected uncertainty in the refined X-ray coordinates is 0.175−0.225 Å, as indicated by the set of dashed theoretical lines (Luzatti, 1952).

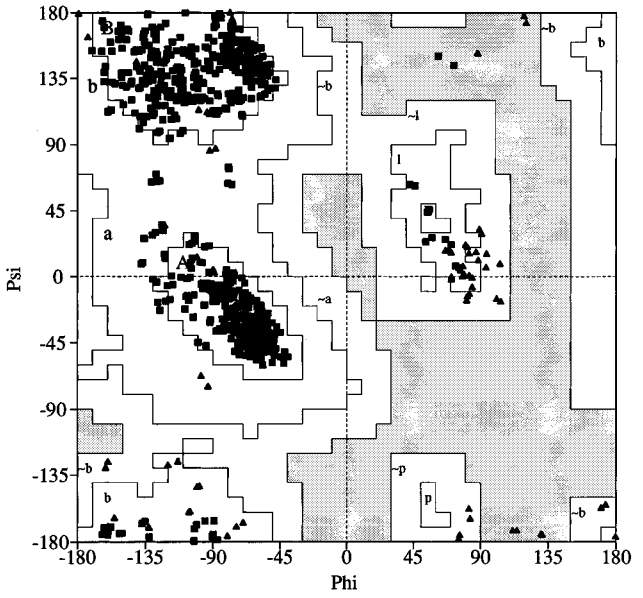

FIGURE 7: Ramachandaran plot of dihedral angles for the H412Q enzyme. The data show that 91.3% of the 892 residues are in the most favored regions (a, b, 1), 8.4% in the additional allowed regions (∼a, ∼b, ∼l, ∼p), and 0.3% in the disallowed regions. Glycine and proline residues are shown as triangles. Asn-293, in both the A and B chains, was the only non-glycine and non-proline residue outside the allows regions. This figure was prepared using PROCHECK (Laskowski et al., 1993).

the most favored or additional allowed regions, as reflected in a Ramachandaran plot of the dihedral angles (Figure 7). The three residues at the N-terminus were not included in the refinement because of very weak electron density.

The major differences between the H412Q and the wild-type structures were detected in the active site region especially at the phosphate binding site and at the mutation site. During the initial refinement, full occupancy of the phosphate site was assumed. Inspection of the electron density maps ($2F_o - F_c$) and the temperature factors suggested that the phosphate was absent and was replaced by two water molecules (Figure 8). The average temperature factors of these waters in the A and B chains were 38 and 26 Å^2, respectively. These two water molecules are hydrogen bonded to the guanidinium nitrogens of Arg-166, the OG1 of Ser-102, and are positioned close to Zn_1, 2.7 and 3.3 Å away, respectively. Arg-166 in the H412Q structure remained in the same position as in the structure of the wild-type enzyme and formed hydrogen bonds with these two water molecules at distances of 2.9 and 3.4 Å. The position of Ser-102 shifted 0.7 Å from the wild-type position away from Zn_2 and toward one of the waters in the phosphate site.

The refined position of Zn_1 in the mutant enzyme was almost the same as its position in the wild-type structure (Kim & Wyckoff, 1991), and this site was almost fully occupied, 0.95 and 0.94 for the A and B chains, respectively. Besides the two waters in the phosphate binding site, another water molecule was within 3.3 Å of Zn_1. The ligands of Zn_1 were well defined and in positions similar to those found in the wild-type structure except for the location of Gln-412. The side chain of Gln-412 flipped away from the position of His-412 in the wild-type structure (Figure 9); however, the OE1 of Gln-412 pointed to Zn_1, although it was too far (3.2 Å) to coordinate. In addition, the side chain Glu-411, coordinated to Ser-381 of the other chain in the wild-type structure, shifted position in order to form a water-mediated interaction with the NE2 of Glu-412 in the same chain.

The Zn_2 site was fully occupied, and the ligands of Zn_2 were in positions almost identical to those in the wild-type structure, except that no phosphate was coordinated to Zn_2 (see Figure 8). Zinc was modeled into the third metal site because analysis of the structural data suggested that the metal in this site had a larger number of electrons than did Mg. A zinc atom with nearly full occupancy refined well at this position, although mixed occupancy of zinc and magnesium at this site could not be ruled out. The introduction of zinc at this site may be an artifact of the relatively high concentrations of zinc used in the crystal stabilization buffer (10 mM).

DISCUSSION

In the catalytic mechanism of *E. coli* alkaline phosphatase, Zn_1 plays a critical role in binding both the substrate and phosphate, in stabilizing the developing negative charge on the leaving group, and in releasing the phosphate product (Kim & Wyckoff, 1991). In previous studies, site-specific mutagenesis was used to replace His-412 by asparagine and alanine (Ma & Kantrowitz, 1994) in order to probe the role of Zn_1 in the mechanism of alkaline phosphatase and to determine the importance of the residues in the coordination sphere of Zn_1. Here, we continue these studies with the mutant enzyme in which His-412 was replaced by glutamine.

The Hydrolysis Activity of the H412Q Enzyme Is Higher Than That of the Wild-Type Enzyme at pH 8. The zinc content of the H412Q enzyme was about half that observed for the wild-type enzyme. However, even in the absence of added zinc, the H412Q enzyme exhibited a hydrolysis activity close to the wild-type levels, although the K_m was almost 50-fold higher than the wild-type value, thus reducing the overall catalytic efficiency of the mutant enzyme. The addition of 0.1 mM Zn^{2+} to the H412Q enzyme resulted in a k_{cat} 1.3-fold higher than the wild-type value; however, even with additional Zn^{2+} the K_m was still 8-fold higher than the wild-type value.

At optimal concentrations of zinc, the K_m and K_i values of the H412Q enzyme decreased, compared to those in the absence of zinc, but were still about 8- and 3-fold higher, respectively, than the corresponding values for the wild-type enzyme (Table 2). These data indicate that the binding of

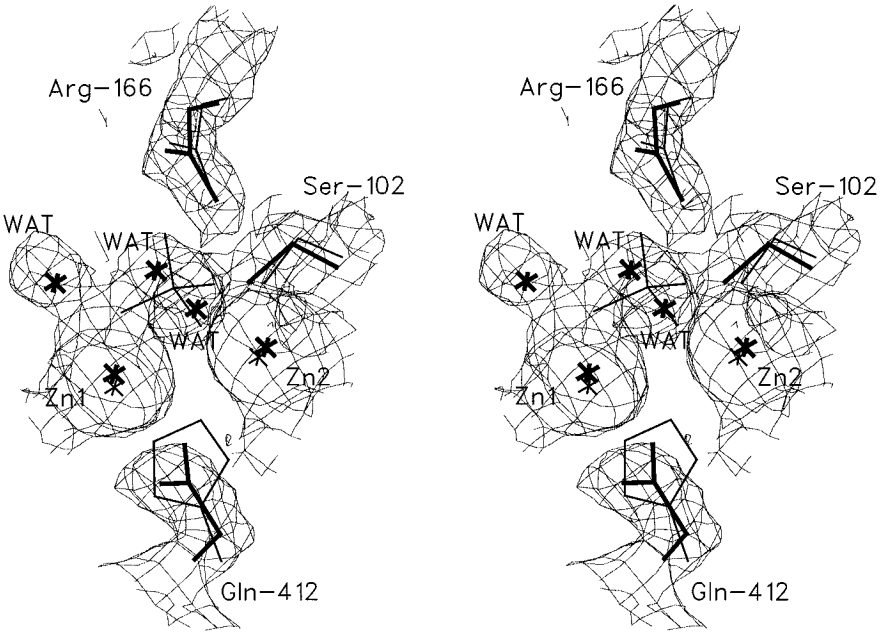

FIGURE 8: Stereoview of the ($2F_o - F_c$) electron density maps ($\sigma = 1.0$) at the Zn_1 and phosphate binding sites for the B subunit of the H412Q enzyme. The refined coordinates of the mutant (thick) and wild-type (thin) structures are superimposed on the electron density. This electron density confirms that the histidine at position 412 has been replaced by glutamine. No phosphate is observed at the phosphate binding site; however, this site is occupied by two water molecules. Another water molecule also is coordinated Zn_1. Figures 8−10 were drawn with the program SETOR (Evans, 1993).

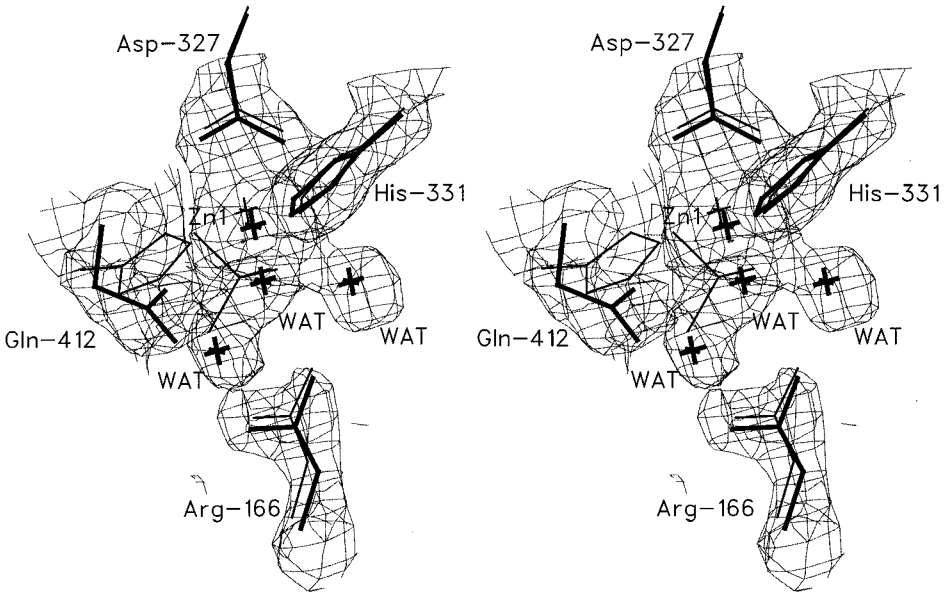

FIGURE 9: Stereoview of the ($2F_o - F_c$) electron display maps ($\sigma = 1.0$) of the H412Q structure showing Zn_1 and its ligands. The refined coordinates of the mutant (thick) and wild-type (thin) structures are superimposed on the electron density.

phosphate is substantially weaker to the H412Q than to the wild-type enzyme. Since the rate-determining step at pH 8 is the dissociation of phosphate from the noncovalent enzyme−phosphate complex, the reduced binding of phosphate to the H412Q enzyme would explain the increased k_{cat} value.

Tris Inhibits the Activity of the H412Q Enzyme. Kinetic studies on the H412Q enzyme indicated that Tris not only functioned less effectively as a phosphoryl acceptor in the transferase reaction but also inhibited the hydrolysis reaction. Tris functioned in an analogous fashion for the H412N and H412A enzymes (Ma & Kantrowitz, 1994). All three mutant enzymes had very low activities in the presence of 1.0 M Tris compared to the wild-type enzyme, but the inhibition by Tris could be overcome by addition of zinc. However, optimal concentrations of zinc restored substrate and phosphate binding almost completely to wild-type levels for the H412N and H412A enzymes but only partially for the H412Q enzyme. These data suggested that the Tris inhibition was related to the altered Zn_1 binding in these mutant enzymes.

NMR experiments on the H412Q enzyme revealed that Tris still functioned as a phosphoryl acceptor in the transferase reaction but at a less effective level, as reflected by the decreased ratio between transferase and hydrolysis activities compared to that of the wild-type enzyme. NMR experiments and kinetic data together showed that Tris inhibited both transferase and hydrolysis reactions and that

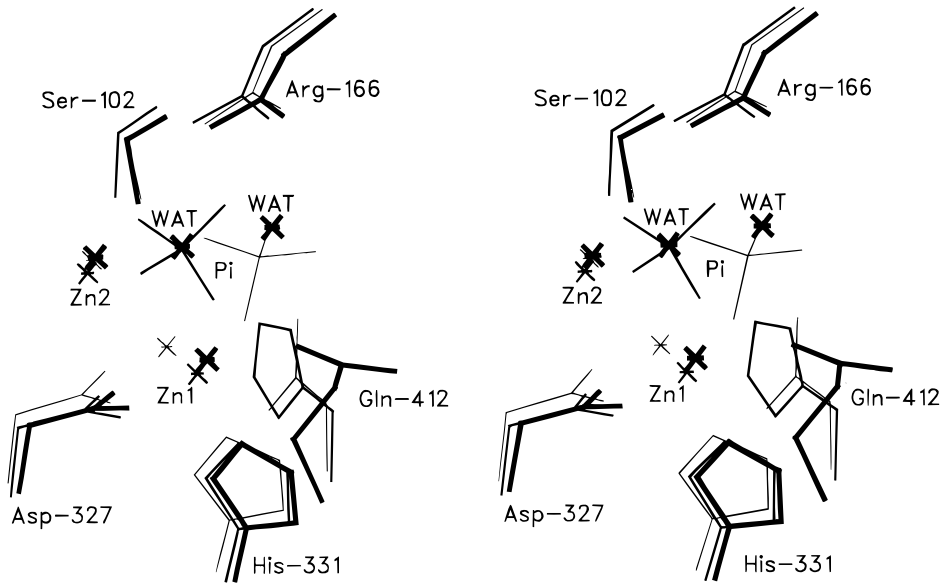

FIGURE 10: Stereoview comparison of the positions of the active site residues in the H412Q (thick line), the wild-type (medium line) (Kim & Wyckoff, 1991), and the H412N(+Zn) (thin line) (Ma et al., 1995) structures.

the inhibition must have occurred before the breakdown of the covalent intermediate (E−P), since the ratios of the transferase to the hydrolysis reactions were independent of the concentrations of zinc or Tris. A possible explanation is that the binding of Tris or another phosphate acceptor further reduced Zn_1 binding, which in turn resulted in a substantial reduction in both the k_{cat} and the K_m values. This interpretation is supported by the fact that the zinc concentration for optimal activity of the H412Q enzyme in 1.0 M Tris is much higher (0.6 mM) than the zinc concentration required for its optimal activity in 0.01 M Tris (0.1 mM).

Glutamine Cannot Replace His-412 as a Direct Ligand to Zn_1, but Zinc Binding Was Not Abolished by the Substitution. The X-ray structure of the H412Q enzyme showed that the side chain of Gln-412 flipped away from the position of the side chain of His-412 in the wild-type structure, with the Gln-412 OE1 atom located 3.2 Å away from Zn_1 (Figure 10). In contrast, previous studies on the structure of the H412N enzyme indicated that Asn-412 was in a similar position as His-412 in the wild-type enzyme (Ma et al., 1995). However, the Asn-412 OD1 atom was 3.1 Å from Zn_1, too far from Zn_1 to interact directly (Figure 10). Although the side chain of glutamine is longer than that of asparagine, in the case of the H412Q enzyme, glutamine does not orient itself in a position that would allow it to be a direct ligand to Zn_1. These observations suggest that the imidazole nitrogen of histidine is critical for coordination to Zn_1, and that the structure of the imidazole ring of histidine is necessary for providing the precise geometry and electrostatics for coordination to Zn_1.

The Gln Substitution at the 412 Site Had a Smaller Effect on Zn_1 Binding Than Did the Asn and Ala Substitutions. The zinc content of both the H412Q and H412N enzymes was lower than that of the wild-type enzyme (Ma & Kantrowitz, 1994); however, the zinc content of the H412Q enzyme was considerably higher than that of the H412N enzyme, even though neither side chain functioned as a direct ligand to Zn_1. In addition, lower concentrations of zinc were required to fully activate the H412Q (0.1 mM) as compared to the H412N enzyme (0.2 mM). In agreement with the kinetic observations, the X-ray structures of these mutant enzymes showed that the Zn_1 site was 20% occupied by zinc in the H412N(+Zn) structure (Ma et al., 1995), while under the same crystallization conditions, the Zn_1 site in the H412Q was almost fully occupied (95%). Furthermore, the position of Zn_1 in the H412N enzyme shifted 1.3 Å compared to the wild-type enzyme, and the ligands to Zn_1 were disordered. In contrast, Zn_1 in the H412Q structure remained in about the same position as in the wild-type structure, and His-331 and Asp-327, the other ligands to Zn_1, were well ordered (Figure 10). These results suggest that even though Gln does not act as a direct ligand to Zn_1, the mutation is better able to fulfill the coordination sphere of Zn_1, compared to the H412N substitution; thus the H412Q enzyme is a better enzyme than either the H412N or the H412A. Both Asn-412 and Gln-412 have their carbonyl oxygens pointed to Zn_1 at a distance of approximately 3.1 Å, which is longer than the usual distance of a coordinating ligand but close enough to fill the coordination sphere of Zn_1. The coordination of Zn_1 in the H412N(+Zn) structure is less complete than that in the H412Q structure, which probably accounts for the higher Zn_1 affinity of the H412Q enzyme compared to the H412N enzyme.

The Glutamine Substitution at Position 412 Locally Alters the Structure of the Enzyme. In the H412Q structure, the side chain of Ser-102 moves approximately 0.7 Å from its position in the wild-type structure and points toward the phosphate binding site, as was observed in the structures of the H412N(+Zn) and H412N(−Zn) enzymes (Ma & Kantrowitz, 1994). This could be a result of the altered Zn_1 sites of these mutant enzymes. The change in the position of Ser-102 may also be due to an alteration in the electrostatic environment of the active sites of the mutant enzymes owing to the amino acid substitutions. The phosphate, which is 2.7 Å from Ser-102 in the wild-type structure, has altered its position as well. In both the H412N(+Zn) and H412N(−Zn) structures, the phosphate moved away from Ser-102 by about 1.7 Å compared to its position in the wild-type structure and was closer to the surface of the enzyme. In contrast to the H412N structures, no phosphate was observed in the active site of the H412Q structure. In the case of the H412Q enzyme, phosphate is not observed in the structure

even though the crystal stabilization buffer had 2 mM P_i, exactly the same as used for the H412N structures. Two water molecules take the place of the phosphate in the H412Q structure, and one of these fills a gap in the coordination sphere of Zn_1.

Inspection of the active site region of the H412Q structure provides an explanation for the observed Tris inhibition of the enzyme. The substitution of Gln for His-412 appears to loosen the coordination sphere around Zn_1, suggesting that Zn_1 binding may be even further reduced when Tris is bound. Alternatively, the replacement of His-412 by other residues, such as Ala, Asn, and Gln, may create an improved binding site for the Tris. Furthermore, since the side chain carbonyl oxygen of Gln-412 in the mutant enzyme is pointing toward Zn_1, there is the possibility that the amide could provide a hydrogen-bonding partner for the hydroxyl oxygens of the Tris, thus providing a possible mechanism for the observed Tris inhibition. The fact that the H412Q enzyme had a more complete Zn_1 coordination sphere than the H412N and H412A enzymes may explain why Tris did not inhibit the H412Q enzyme as much as it did the H412N or H412A enzymes.

Summary. Observations obtained from studies with the H412N and H412A enzymes (Ma & Kantrowitz, 1994) as well as the H412Q enzyme reported here indicate that alkaline phosphatase has a tolerance for substitutions at the 412 position. In the case of the Asn and Gln substitutions at position 412, metal affinities are reduced; however, the addition of zinc to these mutant enzymes does restore enzymatic activity, since His-412 is mainly involved in Zn_1 binding and does not directly participate in catalysis. The catalytic efficiency of the H412Q enzyme is reduced compared to the wild-type enzyme and is directly related to the extent to which the Zn_1 site is occupied. Furthermore, the fact that neither Gln, Asn, nor Ala can effectively replace His-412 as a direct ligand to Zn_1 suggests that the structure and electrostatics of the imidazole ring of histidine are critical for the interaction between the 412 site and Zn_1.

ACKNOWLEDGMENT

We thank D. Robinson for assistance with the atomic absorption experiments, C. Zhou for assistance with the NMR experiments, and T. T. Tibbitts and B. Stec for help in the X-ray structural analysis.

REFERENCES

Anderson, R. A., Bosron, W. F., Kennedy, F. S., & Vallee, B. L. (1975) *Proc. Natl. Acad. Sci. U.S.A. 72*, 2989−2993.

Anderson, R. A., Kennedy, F. S., & Vallee, B. L. (1976) *Biochemistry 15*, 3710−3715.

Bloch, W., & Beckar, D. (1978) *J. Biol. Chem. 253*, 6211−6217.

Bradford, M. M. (1976) *Anal. Biochem. 72*, 248−254.

Brünger, A. T. (1992) *X-PLOR, Version 3.1*, Yale University Press, New Haven, CT.

Chaidaroglou, A., Brezinski, J. D., Middleton, S. A., & Kantrowitz, E. R. (1988) *Biochemistry 27*, 8338−8343.

Coleman, J. E. (1992) *Annu. Rev. Biophys. Biomol. Struct. 21*, 441−483.

Dayan, J., & Wilson, I. B. (1964) *Biochim. Biophys. Acta 81*, 620−623.

Engström, L. (1962) *Biochim. Biophys. Acta 56*, 606−609.

Evans, S. V. (1993) *J. Mol. Graphics 11*, 134−138.

Garen, A., & Levinthal, C. (1960) *Biochim. Biophys. Acta 38*, 470−483.

Hamlin, R., Cork, C., Howard, A., Nielson, C., Vernon, W., Mathews, D., & Xuong, N. h. (1981) *J. Appl. Crystallogr. 14*, 85−93.

Hull, W. E., Halford, S. E., Gutfreund, H., & Sykes, B. D. (1976) *Biochemistry 15*, 1547−1561.

Janeway, C. M. L., Xu, X., Murphy, J. E., Chaidaroglou, A., & Kantrowitz, E. R. (1993) *Biochemistry 32*, 1601−1609.

Kim, E. E., & Wyckoff, H. W. (1991) *J. Mol. Biol. 218*, 449−464.

Kunkel, T. A. (1985) *Proc. Natl. Acad. Sci. U.S.A. 82*, 488−492.

Kunkel, T. A., Roberts, J. D., & Zakour, R. A. (1987) *Methods Enzymol. 154*, 367−382.

Laemmli, U. K. (1970) *Nature 227*, 680−685.

Laskowski, R. A., MacArthur, M. W., Moss, D. S., & Thornton, J. M. (1993) *J. Appl. Crystallogr. 26*, 283−291.

Lowry, O. H., Rosebrough, N. J., Farr, A. L., & Randell, R. H. (1951) *J. Biol. Chem. 193*, 265−275.

Luzatti, P. V. (1952) *Acta Crystallogr. 5*, 802−810.

Ma, L., & Kantrowitz, E. R. (1994) *J. Biol. Chem. 269*, 31614−31619.

Ma, L., Tibbitts, T. T., & Kantrowitz, E. R. (1995) *Protein Sci. 4*, 1498−1506.

Plocke, D. J., & Vallee, B. L. (1962) *Biochemistry 1*, 1039−1043.

Schwartz, J. H., & Lipmann, F. (1961) *Proc. Natl. Acad. Sci. U.S.A. 47*, 1996−2005.

Segel, I. H. (1975) *Enzyme Kinetics*, New York, Wiley.

Simpson, R. T., & Vallee, B. L. (1968) *Biochemistry 7*, 4343−4349.

Sowadski, J. M., Handschumacher, M. D., Murthy, H. M. K., Kundrot, C., & Wyckoff, H. W. (1983) *J. Mol. Biol. 170*, 575−581.

Sowadski, J. M., Handschumacher, M. D., Murthy, H. M. K., Foster, B. A., & Wyckoff, H. W. (1985) *J. Mol. Biol. 186*, 417−433.

Tibbitts, T. T., Xu, X., & Kantrowitz, E. R. (1994) *Protein Sci. 3*, 2005−2014.

Vieira, J., & Messing, J. (1987) *Methods Enzymol. 153*, 3−11.

Wilson, I. B., Dayan, J., & Cyr, K. (1964) *J. Biol. Chem. 239*, 4182−4185.

Xu, X., & Kantrowitz, E. R. (1991) *Biochemistry 30*, 7789−7796.

BI9523421